Spatial Variation of CO Excitation in High-z Galaxies

Chelsea E. Sharon[1], Andrew J. Baker[1], Andrew I. Harris[2], Dieter Lutz[3], Linda J. Tacconi[3], Steven N. Longmore[4], Alasdair P. Thomson[5], Amitpal S. Tagore[1], Charles R. Keeton[1], & Alice E. Shapley[6]

[1]Rutgers, the State University of New Jersey [2]University of Maryland [3]Max-Planck-Institut für extraterrestrische Physik [4]European Southern Observatory [5]University of Edinburgh [6]University of California, Los Angeles

CO in High-z Galaxies

• Observations of CO rotational lines can be used to determine the physical conditions of the molecular gas that fuels star formation.

• Recent CO observations show that submillimeter galaxies (SMGs) have a common CO(3-2)/CO(1-0) line ratio of $r_{3,1}$≈0.6 (in brightness temperature units; e.g., Swinbank et al. 2010; Harris et al. 2010; Ivison et al. 2011; Danielson et al. 2011) indicating the presence of multi-phase molecular gas, including a substantial cold gas reservoir.

• Quasar host galaxies have $r_{3,1}$ closer to unity, indicating they lack the cold molecular gas seen in SMGs, and are well-described by a single-phase molecular ISM (Riechers et al. 2011).

• These results highlight the need for CO spectral line energy distributions (CO SLEDs) to be complete down to the lowest-*J* transition (using instruments like the Zpectrometer; Harris et al. 2007) if we wish to determine high-z galaxies' star formation potential and their likely z~0 descendents.

The Zpectrometer opened up in lab at UMD.

Resolution Effects

• While $r_{3,1}$ is a powerful diagnostic for the presence of a multi-phase molecular ISM, more detailed characterizations of the gas physical conditions require full radiative transfer modeling (e.g., using the Large Velocity Gradient (LVG) approximation; Ward et al. 2003; Weiß et al. 2007).

• In order to be confident about radiative transfer results, we must be certain that the different CO lines are being emitted from the same gas clouds, which may not be the case in complicated sources like major mergers.

• Many studies of high-z sources also exploit the magnification provided by a gravitational lens; differential lensing (the variation in magnification factor across an extended source) could affect observed line ratios.

• Since low spatial and spectroscopic resolution observations can hide complicated source structures, interferometric mapping of the CO SLEDs at high resolution is necessary if we are to determine the gas conditions that accompany the large star formation rates seen in high-z galaxies.

SMM J00266+1708

• J00266 was first detected in the SCUBA Lens Survey (Smail et al. 2002).

• Initial CO observations failed due to an incorrect optically-determined redshift (Frayer et al. 2000).

• Observations of the CO(1-0) line with the Zpectrometer on the Robert C. Byrd Green Bank Telescope confirmed a *Spitzer* PAH redshift estimate (Valiante et al. 2007) of z = 2.742.

• We followed up with observations at the Jansky Very Large Array (VLA) in CO(1-0), at the Plateau de Bure Interferometer (PdBI) in CO(3-2) and CO(5-4), and at the Submillimeter Array in CO(7-6) (Sharon et al. in prep.).

• We discovered a second component in the mid-*J* lines that was undetected by the Zpectrometer (Fig. 1).

• J00266 is likely comprised of two merging galaxies (Fig. 2): a blue component with dispersion-dominated kinematics and a single-phase molecular ISM, and a red component with a velocity gradient and a multi-phase molecular ISM (Fig. 3).

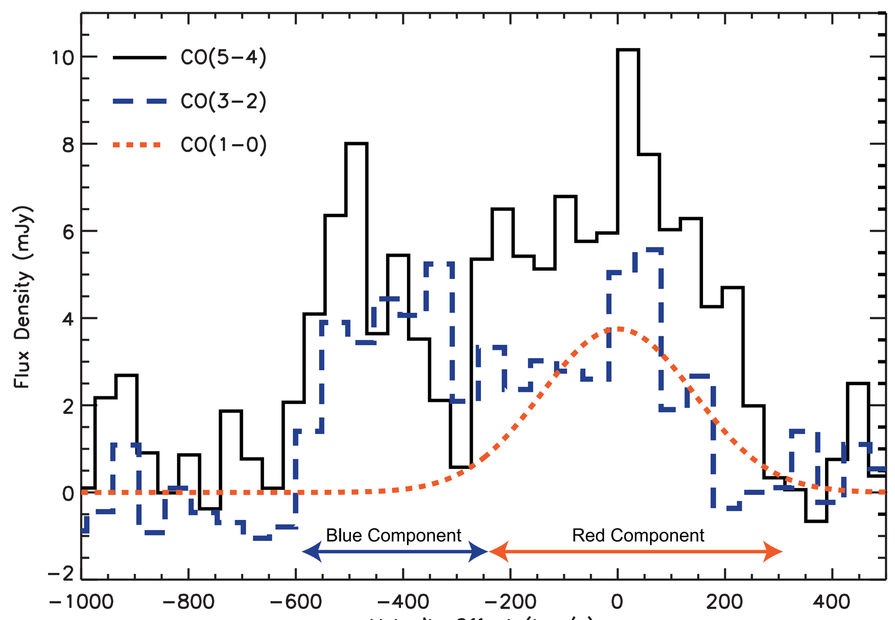

Figure 1- The CO(5-4) (solid/black) and CO(3-2) (dashed/blue) spectral lines, shifted to match the rest frame velocity of the CO(1-0) line (Gaussian fit to GBT observation shown in dotted orange line; multiplied by a factor of five for clarity).

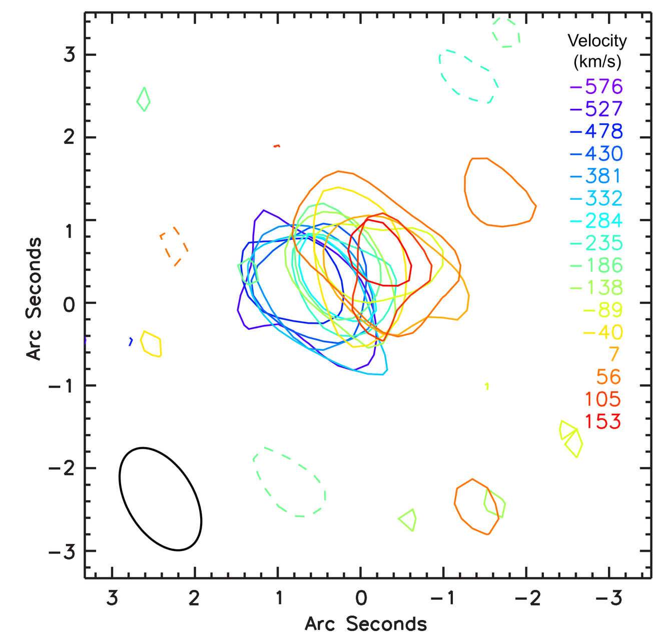

Figure 2- Overlaid contours of the CO(3-2) channel maps, colorized by the channels' relative velocities. The beam size is shown in the lower left corner. Only the positive (solid) and negative (dashed) 3σ contours are shown (σ = 3.6 mJy beam^{-1}).

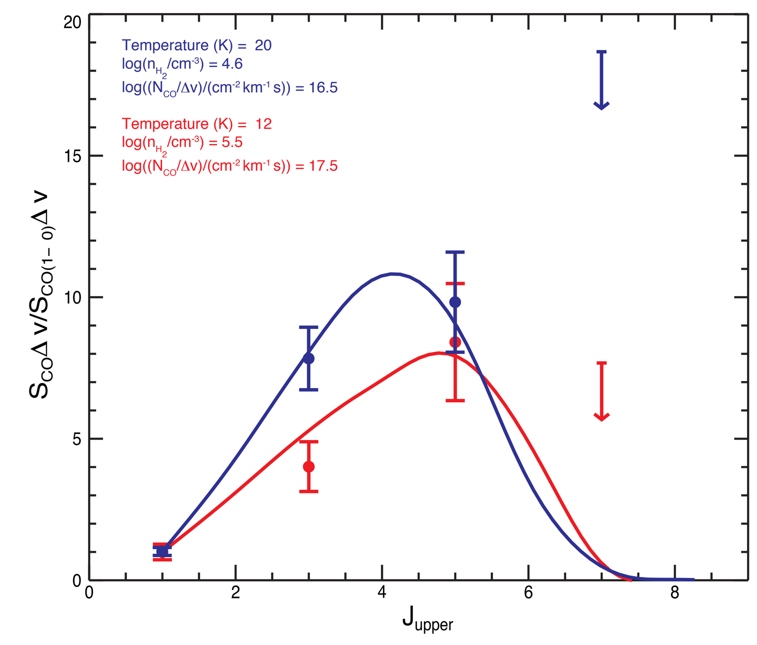

Figure 3- Best fit single-phase CO SLEDs for the blue and red components (solid lines) and the measured line ratios (points; not in brightness temperature units).

SMM J14011+0252

• J14011 (z = 2.5652) was detected in the SCUBA Lens Survey (Smail et al. 2002) and was the first SMG to be detected in any CO line (Frayer et al. 1999).

• J14011 has been followed up extensively at optical wavelengths, including Hα integral field spectroscopy (e.g., Barger et al. 1999; Tecza et al. 2004; Nesvadba et al. 2007).

• Our CO(1-0) detection with the Zpectrometer gave $r_{3,1}$ = 0.76 ± 0.12 (Harris et al. 2010).

• We followed up with mapping of the CO(1-0) line at the VLA (Fig. 4; Sharon et al. in prep.).

• The line ratio maps indicate the presence of an excitation gradient parallel to the lensing shear (Fig. 5).

• While single-phase LVG models (Fig. 6) exist for a range of conditions (lower (higher) T_{kin} models prefer higher (lower) H_2 densities), they favor optically thin emission in the south and optically thick emission in the north (C I observations produce temperatures in line with the southern/optically thin CO emission; Walter et al. 2011).

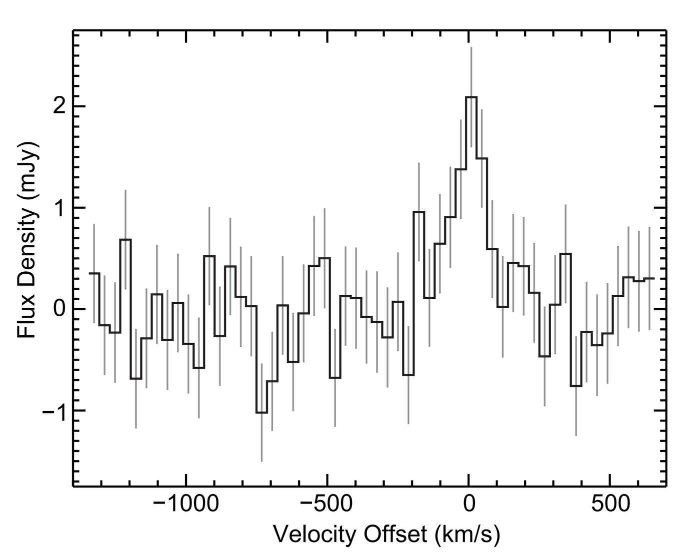

Figure 4- The 37 km s^{-1} resolution VLA spectrum plotted relative to the CO(1-0) systemic redshift. Vertical lines indicate statistical uncertainties.

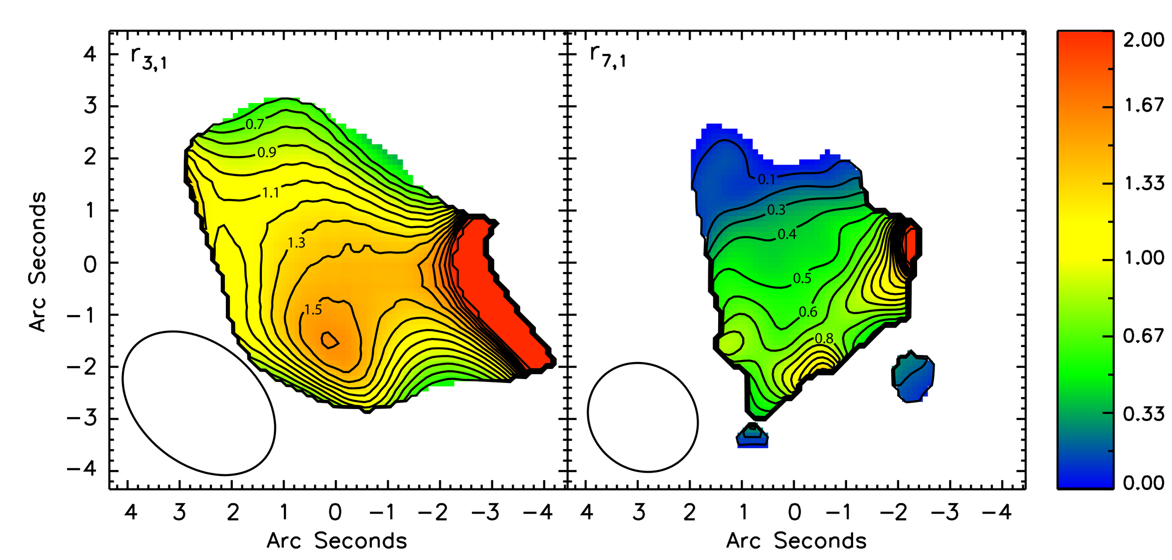

Figure 5- Maps of the CO(3-2)/CO(1-0) (left) and CO(7-6)/CO(1-0) (right) line ratios in units of brightness temperature centered at α (J2000) = 14^{h}01^{m}04.93^s and δ (J2000) = +02°52'24.1". For each panel the CO(1-0) map was first convolved with a Gaussian to give the same resolution as the higher-*J* map (beam sizes are shown in the lower left corners). Pixels with negative line ratios have been blanked out, as are pixels that are not of at least 2σ significance in one of the CO intensity maps. Contours are in steps of 0.1. The color mapping is saturated (and the contouring stopped) at $r_{J,1}$ = 2 for clarity.

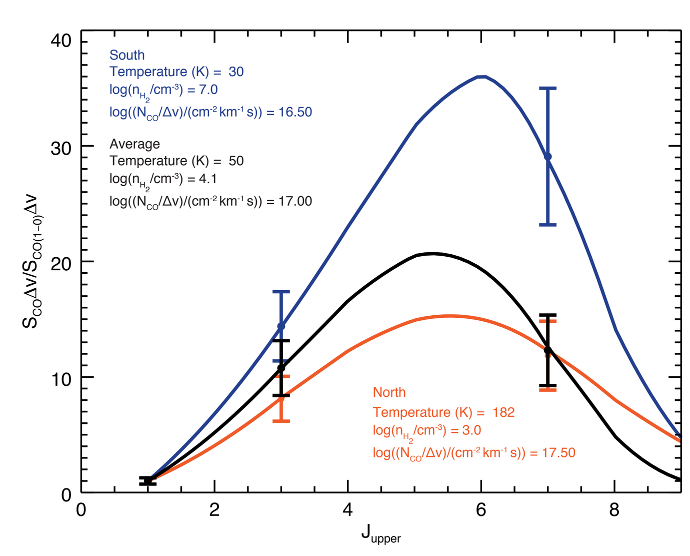

Figure 6- Best fit single-phase CO SLEDs (lines) and line ratios (points; not in brightness temperature units) for the full source (black), for the southern end (blue), and for the northern end (orange).

SDSSJ0901+1814

• J0901 is a strongly lensed star-forming galaxy (z = 2.2597) discovered in a systematic Sloan Digital Sky Survey search (Diehl et al. 2009).

• It is luminous in both rest-UV and dust emission (i.e., J0901 is similar to both Lyman break galaxies and SMGs).

• We observed the CO(3-2) line at the PdBI (Baker et al. in prep.) and the CO(1-0) line at the VLA (Sharon et al. in prep.).

• Clear velocity gradients exist across the three images (Fig. 7) and the preliminary source plane reconstruction indicate that J0901 is a disk galaxy.

• J0901's complex kinematic structure has allowed us to develop a detailed model for the lensing potential (using a non-parametric source reconstruction algorithm developed by A. S. Tagore that provides a major extension to C. R. Keeton's LENSMODEL software).

• While the integrated CO maps place initial constraints on the mass distribution of the lens, this model can be further refined by requiring the lensed images in each velocity channel within the full data-cube to trace back to the same spatial location.

• Differences in the line shape and strengths between the three images indicate that differential lensing may be affecting the source (Fig. 9).

• The CO(3-2)/CO(1-0) line ratio map (Fig. 10) indicates that the lower excitation gas is more spatially extended than the higher excitation gas.

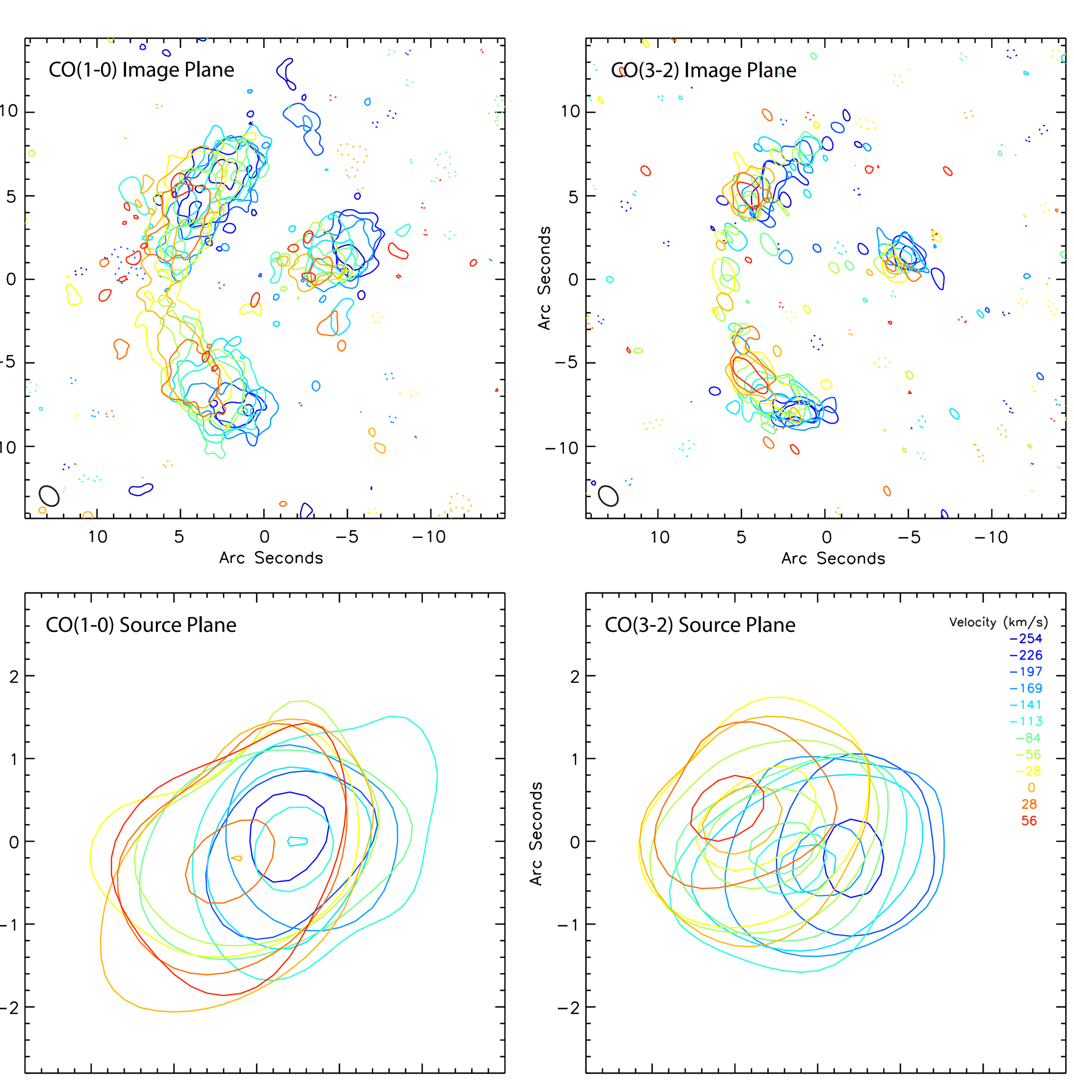

Figure 7- Overlaid contour plots of every other 14 km s^{-1} channel map in our CO(1-0) data cube (top left) and CO(3-2) data cube (top right), and of the corresponding source plane reconstructions (CO(1-0) bottom left, CO(3-2) bottom right). Image plane contours are at ±3σ (σ_{1-0}=0.15 mJy beam^{-1}, σ_{3-2}=0.57 mJy beam^{-1}; these contours do not de-lens exactly to plotted source plane contours). The higher resolution CO(1-0) map was made using a Gaussian restoring beam that matched the CO(3-2) data (shown in lower left corner). In the lensing reconstruction the regularization is held constant, giving the same spatial resolution for both lines (1" in the source plane is equivalent to 8.3 kpc at z=2.2597).

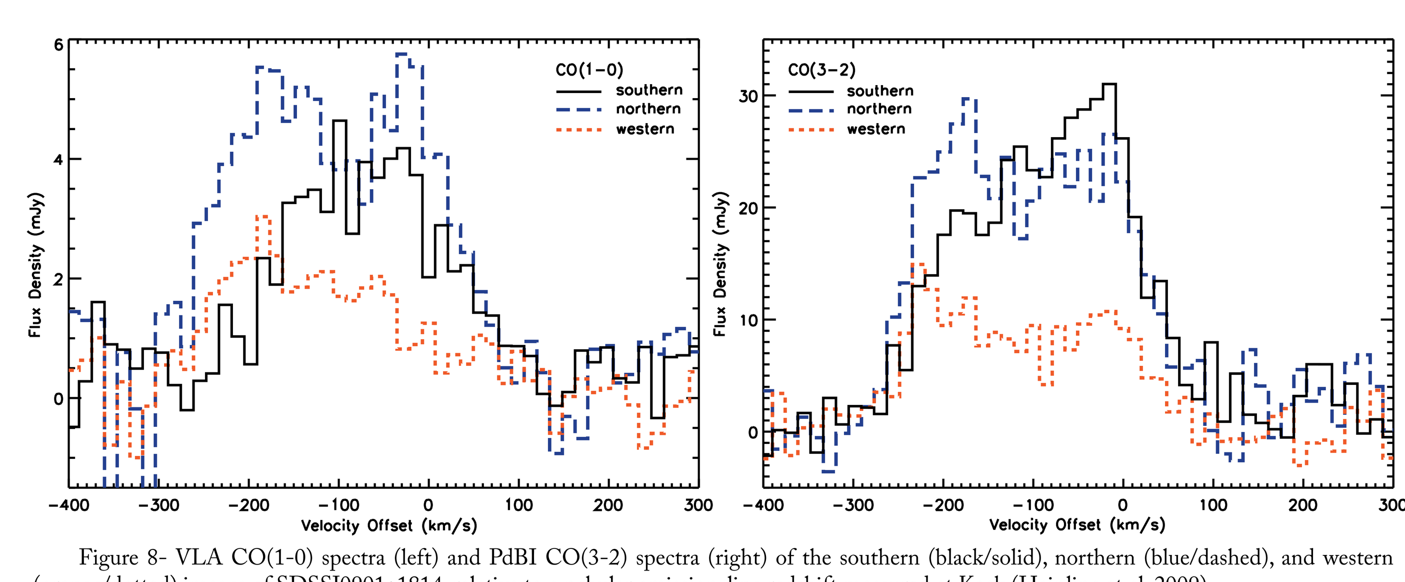

Figure 8- VLA CO(1-0) spectra (left) and PdBI CO(3-2) spectra (right) of the southern (black/solid), northern (blue/dashed), and western (orange/dotted) images of SDSSJ0901+1814, relative to a nebular emission-line redshift measured at Keck (Hainline et al. 2009).

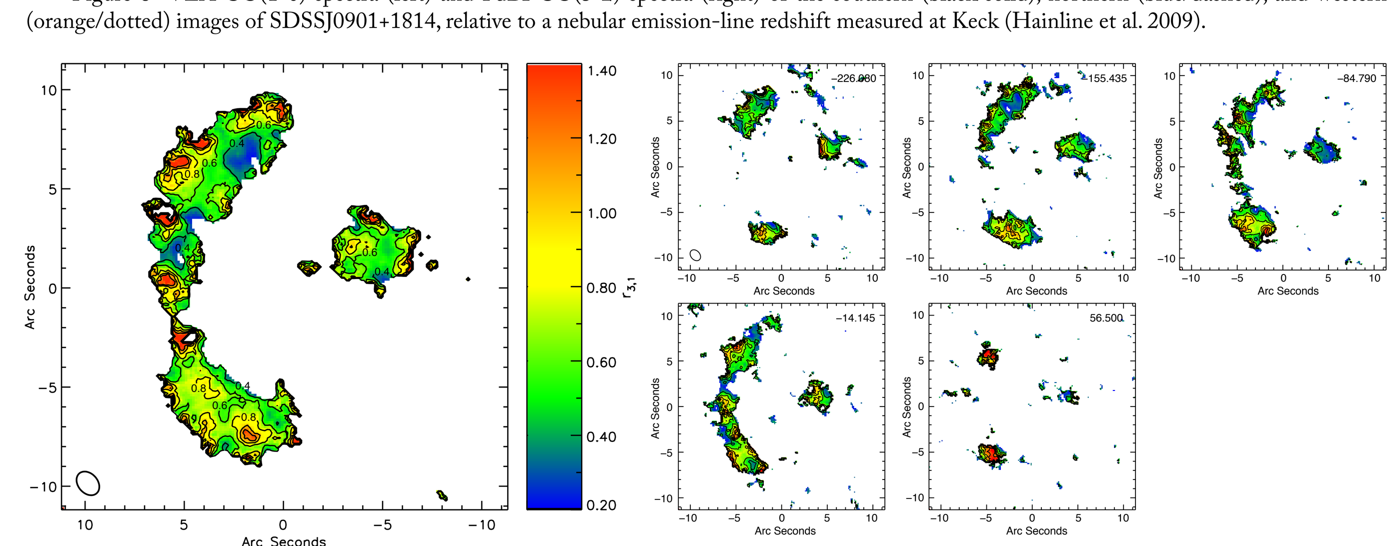

Figure 9- Map of the CO(3-2)/CO(1-0) line ratio in units of brightness temperature for the integrated line (left) and five 71 km s^{-1} channels that span the line width (right). The higher resolution CO(1-0) map was made using a Gaussian restoring beam that matched the CO(3-2) data (shown in lower left corner), and clipped at the same inner uv-radius. As in Fig. 5, negative and <1σ significance pixels have been blanked out, contours are in steps of 0.2, and the color saturation is $r_{3,1}$=1.4.

Conclusions

• Observations of the complete CO excitation ladder, including a cold gas tracer like CO(1-0), are necessary in order to obtain an accurate picture of the molecular gas conditions in high-redshift galaxies.

• In addition, it is crucial that observations be made at high spectral and spatial resolution to ensure that peculiar galaxy structures or gravitational lensing are not affecting the excitation analysis.

• High-resolution mapping of mid- and low-*J* transitions has revealed:

• A SMG that is a clear example of a major merger, where the two components have different kinematic structures and different excitation conditions.

• A SMG with an internal excitation gradient that is strongly confirmed using high-resolution mapping of CO(1-0); our ability to detect the gradient is aided by the coincidental alignment of the gravitational lensing shear.

• A strongly-lensed, UV-selected disk galaxy with a clear spatially extended cold gas phase.

• Similar observations are necessary for a larger number of sources in order to establish how common these structures are in high-z galaxy populations.

References

Baker, A. J. et al. 2012 (in preparation) • Barger, A. J. et al. 1999, AJ, 117, 2656 • Danielson, A. L. R. et al. 2011, MNRAS, 410, 1687 • Diehl, H. T. et al. 2009, ApJ, 707, 686 • Frayer, D. T. et al. 1999, ApJ, 514 L13 • Frayer, D. T. et al. 2000, AJ, 120, 1668 • Hainline, K. N. et al. 2009, ApJ, 701, 52 • Harris, A. I. et al. 2007, ASPCS, 375, 72 • Harris, A. I. et al. 2010, ApJ, 723, 1130 • Ivison, R. J. et al. 2011, MNRAS, 412, 1913 • Nesvadba, N. P. H. et al. 2007, ApJ, 657, 725 • Riechers, D. A. et al. 2011, ApJL, 739, 32 • Sharon, C. E. et al. 2012 (in preparation) • Smail, I. et al. 2002, MNRAS, 331,495 • Swinbank, A. M. et al. 2010, Nature, 464, 733 • Tecza, M. et al. 2004, ApJ, 605, L109 • Valiante E. et al. 2007, ApJ, 660, 1060 • Walter, F. et al. 2011, ApJ, 730, 18 • Ward, J. S. et al. 2003, ApJ, 587, 171 • Weiß, A. et al. 2007, ASPCS, 375, 25

RUTGERS
UNIVERSITY

The authors acknowledge support from NSF grants AST-0503946 and AST-0708653, and thank Steve Sirisky for his contributions to the LVG code.